# Reduced dynamics of a one-dimensional Janus particle

Pavol Kalinay
*Institute of Physics, Slovak Academy of Sciences, Dúbravska cesta 9, 84511 Bratislava, Slovakia*

(Received 16 February 2021; accepted 8 July 2021; published 30 July 2021)

A Janus particle diffusing on a line is considered. Aside from its own driving force $f$ acting forward or backward according to its stochastic orientation, it moves in a position-dependent potential $U(x)$. We propose here the mapping scheme generating the effective generalized Fick-Jacobs equation, describing motion of the particle in the spatial coordinate $x$ only; the orientation is understood as the transverse coordinate. The self-propulsion, driving the system out of equilibrium, is reflected as an additional effective potential $-\gamma(x)$ in the reduced picture. It enables us to understand peculiarities of this system in a handy way. The additionally corrected potential redistributes the confined particles in quasiequilibrium causing their piling at the walls. In periodic asymmetric channels, it acquires a growing contribution, responsible for driving the ratchet effect.

DOI: 10.1103/PhysRevE.104.014608

## I. INTRODUCTION

Active particles moving in confined geometries have attracted the attention of many researchers during the last decade. They can represent living cells, e.g., bacteria moving by their own propulsion [1–4], or artificially prepared Janus particles [5–9], coated partially by an active layer reacting with surrounding solvent, pushing the particle forward. Finally, their behavior is also determined by the confining boundaries.

Aside from the important practical use in technologies, the models of Janus particles represent a challenge for the theory of nonequilibrium thermodynamics. The self-propulsion of the particles works as a kind of perturbation, driving the system out of the equilibrium. Together with specific properties of the confinement, it can give rise to interesting states of the matter [9–11], self-organization, or rectification of the stochastic motion of the particles, the ratchet effect [12–17].

One of the simplest models of Janus particles is depicted in Fig. 1(a). The disk of diameter $a$ coated partially by an active (red) layer can represent Ozin's nanoparticles [8] with platinum droplets, immersed in the solution of hydrogen peroxide. The platinum catalyzes the chemical reaction $2H_2O_2 \rightarrow 2H_2O + O_2$ on the droplet surface, which moves the particle in the opposite direction by the force $f$, which is considered here constant in magnitude. However, its direction depends on the particle's orientation, the angle $\phi$ in Fig. 1(a), which changes randomly with the rotational diffusion constant $D_r$. Aside from the rotation and self-propulsion, the particle diffuses inside a confined region [it is here a two-dimensional (2D) channel bounded by the reflecting boundaries at $y = h(x)$ and 0] with the intrinsic translation diffusion constant $D_0$. We also neglect the diameter $a$ of the disk in our considerations, supposing that it is much smaller than the typical length of the channel, say, the width $h(x)$.

The question is analysis of the dynamics of such a system, explaining the observed effects like piling the particles at the boundaries, or rectification of their motion. For passive particles diffusing in quasi-one-dimensional (1D) nonhomogeneous channels, the techniques of dimensional reduction appeared useful [18–27]. The 2D or three-dimensional (3D) diffusion equation was integrated over the cross section and the resulting 1D equation described the dynamics only in the longitudinal direction. Reflecting also nonhomogeneity in the transverse directions, it enabled us to analyze the corresponding effects, like dependence of the effective diffusivity or mobility on the varying profile.

In this paper, we propose to perform a similar mapping on the system of Janus particles. Instead of the spatial transverse coordinates, we integrate here the corresponding equations over the orientation of the particle (and the force $f$). The final reduced equation will describe the motion of the particles solely in the spatial coordinates, but including the effects of their randomly oriented self-propelling force. We expect that the form of the reduced equation will point to the specific behavior of the Janus particles in an easier way.

To explain the dimensional reduction, which is our main aim, we consider here only a simpler 1D version of this model, described in Fig. 1(b). Our particle diffuses along the $x$ axis, but in a potential $U(x)$. Only two possible orientations remain, pushing the disk forward (+) or backward (−); they are flipping randomly with a rate constant $\alpha$, which is an analog to the rotational diffusion constant $D_r$. The probability densities $p_\pm(x,t)$ of the particles facing to the right and left satisfy the Smoluchowski equations with the corresponding potentials $U(x) \mp fx$ coupled by the flipping term $\sim\alpha$,

$$\partial_t p_\pm(x,t) = D_0 \partial_x e^{-\beta[U(x)\mp fx]} \partial_x e^{\beta[U(x)\mp fx]} p_\pm(x,t) \mp \alpha[p_+(x,t) - p_-(x,t)]. \tag{1.1}$$

The inverse temperature $\beta = 1/k_B T$ will be set to 1. The same equations also describe behavior of a passive particle driven by the random force of a constant magnitude $f$, i.e., the fluctuating force ratchet [28].

 

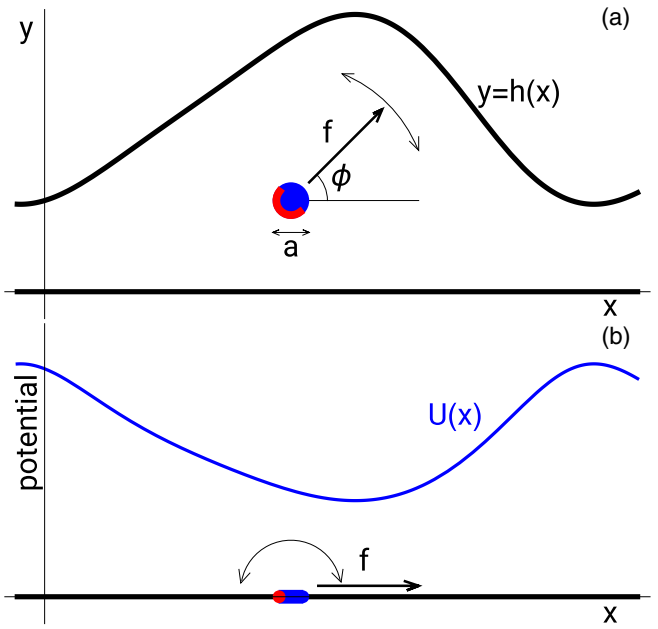


FIG. 1. (a) Scheme of a Janus disk diffusing in a 2D channel. The self-propelled force $f$ drives the disk in an arbitrary direction depending on its stochastic rotation in angle $\phi$. (b) The simplified 1D version of this model in the potential $U(x)$.

Our aim is to find the mapped equation for the density of particles $p(x,t)$ of both orientations. This is a task very similar to the mapping of 2D diffusion [19–24] onto the longitudinal coordinate, where the role of the transverse coordinate is played now by orientation of the disks. Fast flipping ($\alpha \to \infty$) corresponds to a large transverse diffusion constant, providing almost immediate transverse equilibration, generating the Fick-Jacobs (FJ) equation [18]. Then the small parameter here is $\tau \sim D_0/\alpha$; it can control a similar procedure as that formulated for the mapping of the 2D diffusion [21–23]. It generates a series of corrections to the mapped equation expanded in $\tau$, expressing the influence of a nontrivial $U(x)$ onto the dynamics of the flipping self-propelled particle.

We show that the result of the mapping has again the form of the generalized FJ equation,

$$\partial_t p(x,t) = D_0 \partial_x A(x)[1 - \hat{Z}(x,\partial_x)]\partial_x \frac{p(x,t)}{A(x)}, \tag{1.2}$$

with an operator $\hat{Z}$ involving the corrections to the FJ equation expanded in $\tau$. It can be simplified to

$$\partial_t p(x,t) = \partial_x A(x) D(x) \partial_x \frac{p(x,t)}{A(x)}, \tag{1.3}$$

valid in the limit of the stationary solutions [23]; $D(x)$ denotes the spatially dependent effective diffusion coefficient $D(x)$, and the function $A(x)$ is the local Boltzmann factor of the effective potential. Unlike the mapped equations for passive particles diffusing in conservative fields [25–27], also $A(x)$ has to be corrected within the recurrence mapping technique [29]. Finally, it contains a part of the effective potential, which can break the symmetry (periodicity) of a periodic channel and cause (or visualize) the ratchet effect [30].

The mapping presented here deals with a 1D model, where $U(x)$ represents the real potential. Nevertheless, one can also interpret $U(x) = -\ln[h(x)]$ as the entropic potential in a 2D channel of varying width $h(x)$ [Fig. 1(a)]. Then Eq. (1.1) becomes a pair of FJ equations coupled by flipping between (+) and (−) orientations. Of course, such description of the 2D models is only the zero-order approximation of the mapping over the transverse coordinate $y$. The higher corrections of the FJ equations for the separate orientations could be derived by the procedure formulated, e.g., in Ref. [25], but it does not include the flipping terms, which also influence the mapping. Having no scheme yet generating consistently the higher-order corrections, the FJ approximation is often used for the basic description of the 2D models [13,31–34], too. The purpose of this paper is to focus our attention on the mapping over the orientation first, which could also help us to go beyond the FJ description in more complex models.

For the 1D model analyzed here, the mapping over orientation is very simple and convenient to demonstrate the method. In Sec. II, we describe the mapping procedure for the general analytic function $U(x)$. The alternative method, generating directly the functions $A(x)$ and $D(x)$ of the generalized FJ equation (1.3) in the stationary limit, is added in the Appendix. The results for some trial potentials are presented in Sec. III. We exploit the proposed methods to study piling of the Janus particles at the walls and also the ratchet effect in periodic but asymmetric channels. The leading term of the rectified current $\sim 1/\alpha^3$ can be even determined analytically for certain potentials by the first method. On the other hand, the equations obtained in the stationary limit enable us to find the effective diffusion coefficient and the effective force driving the ratchet effect expanded in $f^2$ in the full range of the flipping rates.

## II. MAPPING PROCEDURE

We present here the mapping procedure for the 1D system defined above, following the same steps as applied in the dimensional reduction of diffusion in a 2D channel [21]. Our transverse coordinate now is orientation of the particle, so the first step, integration over the transverse coordinate, is simply summation of Eq. (1.1) over two states (+) and (−),

$$\partial_t p(x,t) = D_0 \partial_x e^{-U(x)}[e^{fx}\partial_x e^{-fx+U(x)} p_+(x,t) + e^{-fx}\partial_x e^{fx+U(x)} p_-(x,t)]; \tag{2.1}$$

$$p(x,t) = p_+(x,t) + p_-(x,t) \tag{2.2}$$

is the marginal density. The energy and time are measured in units such that the temperature $k_B T = 1$ and also $D_0 = 1$ in our next calculations.

Reducing the orientation, the FJ approximation corresponds to the infinitely fast flipping between both orientations, $\alpha \to \infty$, hence they are equally probable, $p_\pm(x,t) = p(x,t)/2$. Indeed, substituting it in Eq. (2.1), we find the Smoluchowski equation,

$$\partial_t p(x,t) = \partial_x e^{-U(x)} \partial_x e^{U(x)} p(x,t). \tag{2.3}$$

[We can also understand it as the FJ equation, where $e^{-U(x)} = h(x)$ means the Boltzmann weight of the potential $U(x)$, either real or entropic.]

If the flipping is slower ($\alpha$ is finite), the particle has time to move before the next flip. Its shift depends on whether it is self-propelled uphill or downhill on the landscape $U(x)$. The probability densities $p_+(x,t)$ and $p_-(x,t)$ are enriched differently by the particles coming from the neighboring positions, so they start to differ from one another. Similar to reducing the transverse spatial coordinates [21,22,25], the deviations of $p_\pm$ from $p/2$ can be formally expressed using the marginal probability density $p(x,t)$. Applying the homogenization method starting with the zero-order solution $p_\pm = p/2$, they have the form of some spatial operators $\omega_\pm(x,\partial_x)$ acting on $p(x,t)$ in general. Without loss of generality, we can write the relation of the backward mapping as

$$p_\pm(x,t) = e^{-U(x)+\gamma(x)}\left[\frac{1}{2} + \hat{\omega}_\pm(x,\partial_x)\right]\frac{p(x,t)}{A(x)}, \tag{2.4}$$

where $A(x)$ is the Boltzmann weight of an effective potential, as introduced in the FJ equation. Inspired by the mapping of diffusion driven by the vortex forces [29], we inserted here the gauge function $\gamma(x)$, which enables us later to bring the mapped equation to the form (1.2). The functions $A(x)$ and $\gamma(x)$, as well as the operator $\hat{\omega}$, are unfixed yet; their derivation is the core of the mapping procedure. Consistency with Eq. (2.2) for any solution $p(x,t)$ (normalization condition) requires us to put $\hat{\omega}_+(x,\partial_x) = -\hat{\omega}_-(x,\partial_x) = \hat{\omega}(x,\partial_x)$ and

$$A(x) = e^{-U(x)+\gamma(x)}. \tag{2.5}$$

Applying relations (2.4) and (2.5) in Eq. (2.1), we arrive at the mapped equation

$$\partial_t p(x,t) = \partial_x A(x)[\partial_x + \gamma'(x) - 2f\hat{\omega}(x,\partial_x)]\frac{p(x,t)}{A(x)} \tag{2.6}$$

after some algebra. As it will be seen later, a part of the operator $\hat{\omega}$ is just a function, not containing $\partial_x$. To convert Eq. (2.6) to the form (1.2), we need to eliminate it by a proper choice of the gauge function $\gamma(x)$. Comparing the right-hand sides of both mentioned equations, we obtain

$$\gamma'(x) + \hat{Z}(x,\partial_x)\partial_x = 2f\hat{\omega}(x,\partial_x) = 2f[\omega(x) + \tilde{\omega}(x,\partial_x)\partial_x]; \tag{2.7}$$

i.e., having $\hat{\omega}$ split into the parts containing and not containing $\partial_x$, its purely functional part $\omega(x)$ fixes the gauge function $\gamma(x)$ and the rest operator $\tilde{\omega}$ determines the corrections $\hat{Z}$ to the FJ equation (2.3).

The deviations of $p_\pm$ from $p/2$ are controlled by the flipping rate $\alpha$. As analyzed before, the ratio $\tau = D_0/2\alpha = 1/2\alpha$ plays here the same role as the small parameter $\epsilon$, scaling the transverse diffusion constant with respect to $D_0$, in reducing the spatial coordinate $y$ in 2D channels [21–23,25,29]. So to apply the homogenization, we can do the same step, to expand the operators $\hat{\omega}$, $\hat{Z}$, as well as the function $\gamma(x)$ in $\tau$,

$$\begin{aligned}\hat{\omega}(x,\partial_x) &= \sum_{n=1}^{\infty}\tau^n\hat{\omega}_n(x,\partial_x)\\ &= \sum_{n=1}^{\infty}\tau^n[\omega_n(x) + \tilde{\omega}_n(x,\partial_x)\partial_x],\\ \hat{Z}(x,\partial_x) &= \sum_{n=1}^{\infty}\tau^n\hat{Z}_n(x,\partial_x) = 2f\sum_{n=1}^{\infty}\tau^n\tilde{\omega}_n(x,\partial_x),\end{aligned}$$

$$\gamma'(x) = \sum_{n=1}^{\infty}\tau^n\gamma_n'(x) = 2f\sum_{n=1}^{\infty}\tau^n\omega_n(x). \tag{2.8}$$

The procedure fixing recursively the coefficients $\hat{\omega}_n$, $\hat{Z}_n$, and $\gamma_n'$ is obtained after substituting the backward mapping relation (2.4) with (2.8) in Eq. (1.1) [say, for the (+) orientation],

$$2\alpha e^{\gamma}\hat{\omega}\frac{p}{A} = [e^U\partial_x e^{-U}(\partial_x - f) - \partial_t]e^{\gamma}\left(\frac{1}{2} + \hat{\omega}\right)\frac{p}{A}, \tag{2.9}$$

omitting writing the obvious arguments. It has to be satisfied for any solution of the reduced problem $p(x,t)$, so it is an operator equation determining $\hat{\omega}$. The time derivative $\partial_t$ commutes here with all spatial operators and acts only on $p(x,t)$, where we apply the mapped equation (1.2). (Any operator automatically acts on anything to the right without explicit writing of brackets in our notation.) We use now the expansions (2.8) and collect the terms of the same order in $\tau$ on both sides. Then having expressed $\hat{\omega}_n$, the coefficients $\hat{Z}_n$ and $\gamma_n'$ are calculated according to Eq. (2.7).

The leading correction is given by the terms $\sim\tau^0$. In the zeroth order, $\hat{\omega}$, $\hat{Z}$, and $\gamma$ on the right-hand side do not contribute and $A(x)$ enters here only as $e^{-U(x)}$, so

$$\begin{aligned}\hat{\omega}_1 &= e^U\partial_x e^{-U}(\partial_x - f)\frac{1}{2} - \frac{1}{2}e^U\partial_x e^{-U}\partial_x\\ &= -\frac{f}{2}\partial_x + \frac{f}{2}U'.\end{aligned} \tag{2.10}$$

The functional and the operator parts of the result can be easily identified; hence, applying Eq. (2.7), we have

$$\gamma_1' = f^2U', \quad \hat{Z}_1 = -f^2. \tag{2.11}$$

In the higher orders, the complexity grows quickly especially because of the presence of $e^{\gamma}$, also contained in $A(x)$. The explicit integration of $\gamma'(x)$ within the recurrence procedure is not necessary. After completing commutations of $e^{\gamma(x)}$, only the derivatives of $\gamma(x)$ remain in the recurrence formulas in any order. As an example, we also state here the equation $\sim\tau^1$,

$$\begin{aligned}\hat{\omega}_2 &= e^U\partial_x e^{-U}(\partial_x - f)\hat{\omega}_1 + e^U\partial_x e^{-U}\frac{\gamma_1'}{2} + \gamma_1'(\partial_x - f)\frac{1}{2}\\ &\quad + \frac{1}{2}e^U\partial_x e^{-U}\hat{Z}_1\partial_x - \frac{\gamma_1'}{2}\partial_x - \hat{\omega}_1 e^U\partial_x e^{-U}\partial_x\\ &= \frac{1}{2}(-f^3U' + fe^U\partial_x e^{-U}U''),\end{aligned} \tag{2.12}$$

giving

$$\begin{aligned}\gamma_2' &= -f^4U' + f^2\big(U^{(3)} - U'U''\big),\\ \hat{Z}_2 &= f^2U''.\end{aligned} \tag{2.13}$$

Finally, the result in $\tau^2$ is more complicated,

$$\begin{aligned}\gamma_3' &= f^6U' - f^4\big(2U^{(3)} - 5U'U'' + U'^3\big) + f^2(U^{(5)}\\ &\quad - 2U'U^{(4)} - 3U''U^{(3)} + U'^2U^{(3)} + U'U''^2),\\ \hat{Z}_3 &= f^4\partial_x^2 + (2f^2U^{(3)} - 3f^4U')\partial_x + 3f^4(U'^2 - U'')\\ &\quad + f^2(3U^{(4)} - 3U'U^{(3)} - U''^2),\end{aligned} \tag{2.14}$$

but necessary for our next considerations.

First, notice that $\hat{Z}_3$ is not just a function, but it also contains the derivatives $\partial_x$, $\partial_x^2$. To avoid problems with solving the higher-order differential equations, we replace Eq. (1.2) by Eq. (1.3), valid in the limit of stationary flow, when the time changes of $p(x,t)$ (and all related quantities) are small [23]. Both equations represent the 1D mass conservation, so both right-hand sides express the derivative of the net flux, $-\partial_x J(x,t)$. For $p(x,t)$ independent of time, $J$ is constant. Comparing the stationary $\partial_x(p/A)$ expressed from

$$J = -A[1-\hat{Z}]\partial_x(p/A), \quad J = -AD\partial_x(p/A), \tag{2.15}$$

we find the relation

$$\frac{1}{D(x)} = A(x)[1-\hat{Z}(x,\partial_x)]^{-1}\frac{1}{A(x)}, \tag{2.16}$$

enabling us to calculate the effective diffusion coefficient $D(x)$, which is just a function, from $\hat{Z}$. Applying our formulas for the first three coefficients $\hat{Z}_n$, we obtain the expansion correct up to third order,

$$\begin{aligned}\frac{1}{D(x)} = 1 &- \tau f^2 + \tau^2 f^4 - \tau^3 f^6 + \cdots + \tau^2 f^2 U'' \\ &+ \tau^3 f^2[f^2(U'^2 - 4U'') + 3U^{(4)} - U'U^{(3)} \\ &- U''^2] + \cdots . \end{aligned} \tag{2.17}$$

Next, the function $-\gamma(x)$ can be interpreted as an extra effective potential, which is added to the real potential $U(x)$, due to random self-propulsion of the particles in a nontrivial confinement; then $\gamma'(x)$ is the additional local effective force. It is worth now to integrate $\gamma_n$ from Eqs. (2.11), (2.13), and (2.14) and to express the new potential, $U(x)$ corrected by the effective contributions from the self-propelling force,

$$\begin{aligned}U(x) - \gamma(x) = (1 &- \tau f^2 + \tau^2 f^4 - \tau^3 f^6 + \cdots)U(x) \\ &- \tau^2 f^2 (U'' - U'^2/2) + \tau^3 \Bigg[ f^4 \Bigg( 2U'' - 5U'^2/2 \\ &+ \int U'^3 dx \Bigg) - f^2 \Bigg( U^{(4)} - 2U'U^{(3)} - U''^2/2 \\ &+ U'^2 U'' - \int U'U''^2 dx \Bigg) \Bigg] + \cdots . \end{aligned} \tag{2.18}$$

Formula (2.17) shows that the effective diffusion coefficient increases due to random self-propulsion of the particles, as expected; the terms independent of the potential give $D(x) = (1 - \tau f^2 + \tau^2 f^4 - \cdots)^{-1} = 1 + f^2/(2\alpha)$. Here $f^2/(2\alpha)$ could be interpreted as the generalized Taylor dispersion [35], being quadratic in the self-propelling force and proportional to variance of the time spent in each orientation [36]. Similar terms in Eq. (2.18) effectively decrease the confining potential $U(x)$ by the factor $1/[1 + f^2/(2\alpha)]$. It enables the particles to access the positions closer to the (soft) walls, what indicates their piling there.

It is difficult to give a simple interpretation of the other terms in $1/D(x)$, or $\gamma(x)$; it is rather useful to study their influence in specific potentials for more details. The most interesting terms in Eq. (2.18) are those unintegrable explicitly for the general $U(x)$, appearing in the order $\sim\tau^3$. In periodic but asymmetric potentials, they can give a nonzero increment $\Delta\gamma = \gamma(L) - \gamma(0)$ over one period $L$, i.e., an effective mean force $\Delta\gamma/L$ driving the particle along the channel and thus visualizing the ratchet effect. We study these effects on trial potentials in the next section.

## III. RESULTS FOR TRIAL POTENTIALS

The mapping procedure presented in the previous section proved that the reduced dynamics of the 1D Janus particles diffusing in a potential $U(x)$ is described by the generalized FJ equation (1.3) with the spatially dependent diffusion coefficient $D(x)$, Eq. (2.17), and $A(x)$ given by Eq. (2.5) with $U(x)$ corrected by the new effective contribution $-\gamma(x)$, Eq. (2.18). Both effective functions are calculated within the recurrence scheme controlled by the small parameter $\tau = 1/2\alpha$; i.e., they are expected to work mainly in the limit of high flipping rates $\alpha$. For smaller $\alpha$, the results are problematic especially if these functions are expressed as truncated series.

However, as shown in the Appendix, knowing already the structure of the dimensional reduction we can modify the mapping technique in the limit of stationary flow to arrive directly at the couple of equations for $\gamma(x)$ and $D(x)$, Eqs. (A5) and (A10), avoiding expansion in $\tau$. Their solutions represent summation of at least some group of the terms in Eqs. (2.18) and (2.17) up to infinity, thus extending their validity also for smaller $\alpha$. For our purposes, we need here mainly Eq. (A5), determining $\gamma(x)$,

$$2\alpha\partial_x e^{\gamma(x)} = e^{U(x)}\partial_x e^{-U(x)}\left(\partial_x^2 - f^2\right)e^{\gamma(x)}. \tag{3.1}$$

Reducibility of the dynamics of any quasi-1D system onto the generalized FJ equation (1.2) implies existence of two important time-independent states: (quasi)equilibrium, when the density $p_{\rm eq}(x) \sim A(x)$, and the stationary flow with constant net flux $J$, Eq. (2.15). The equilibrium can describe piling of the particles at the walls, and the stationary flow calculated in a periodic but asymmetric potential $U(x)$ uncovers the ratchet effect.

We demonstrate the piling on the quadratic potential $U(x) = x^2$, which enables us to determine $\gamma(x)$ analytically up to an arbitrary order in $f^2$. The coefficients $E_n(x^2)$ of $e^{\gamma}$ expanded in $f^2$ are polynomials of the $n$th order, which can be fixed after substitution in Eq. (3.1). Then the system of recurrence algebraic equations gives

$$\begin{aligned}e^{\gamma} = 1 &+ \frac{f^2 x^2}{2(\alpha+1)} + \frac{f^4}{8(\alpha+1)(\alpha+3)}\left(x^4 - \frac{2\alpha x^2}{\alpha+1}\right) \\ &+ \cdots , \end{aligned} \tag{3.2}$$

which is the exact result in any order of $f^2$.

The effective potential $U(x) - \gamma(x)$, determining the equilibrium $p_{\rm eq} \sim e^{-U+\gamma}$, is depicted in Fig. 2. The function $\gamma(x)$ decreases the real potential $U(x)$ for any parameters $f$ and $\alpha$; i.e., it enables the particles to get further from the center, uphill on the soft parabolic wall. For sufficiently strong forces $f$ and small $\alpha$, the effective potential $U - \gamma$ becomes a double well; the particles are piled at the slope, pushed there by their self-propulsion until their orientation is randomly changed. Then they diffuse to the opposite side, piling at the symmetric position $x \to -x$. Of course, this process is effective especially for smaller $\alpha$, when the probability of flipping of their orientation during the way across the potential well is lower.

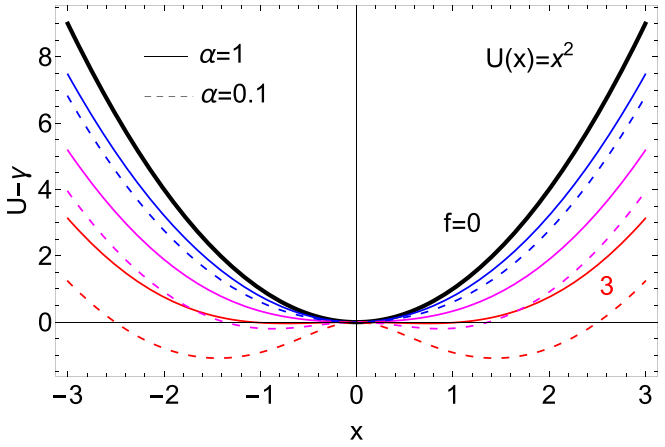


FIG. 2. Effective potential $U(x)-\gamma(x)$ for the quadratic well $U(x)=x^2$ (thick black line) according to Eq. (3.2) (derived up to $f^{16}$ order). The solid and dashed lines represent $\alpha=1$ and $\alpha=0.1$, respectively. The lines (downward) are calculated for $f=1$ (blue), 2 (magenta), and 3 (red).

Our method also enables us to calculate the densities $p_\pm(x)$ and fluxes $j_\pm(x)$ of the particles facing to the right and left. Using the backward mapping (2.4), we have

$$p_\pm = e^{-U+\gamma}\left(\frac{1}{2}\pm\hat{\omega}\right)\frac{p_{\rm eq}}{A} = e^{-U+\gamma}\left(\frac{1}{2}\pm\omega(x)\right)\frac{p_{\rm eq}}{A}$$
$$= e^{-U}\left[e^{\gamma}\pm\frac{1}{f}(e^{\gamma})'\right]\frac{p_{\rm eq}}{2A}. \tag{3.3}$$

The operator $\hat{\omega}(x,\partial_x)$ acting on the constant $p_{\rm eq}/A$ leaves only its functional part $\omega(x)$ nonzero and it is related to $\gamma'(x)=2f\omega(x)$ according to Eq. (2.7). Now the corresponding fluxes can be expressed, too:

$$j_\pm = -e^{-U\pm fx}\partial_x e^{U\mp fx}p_\pm$$
$$= -e^{-U}(\partial_x\mp f)\left[e^{\gamma}\pm\frac{(e^{\gamma})'}{f}\right]\frac{p_{\rm eq}}{2A}$$
$$= \pm e^{-U}\left[fe^{\gamma}-\frac{1}{f}(e^{\gamma})''\right]\frac{p_{\rm eq}}{2A}. \tag{3.4}$$

The plots of $p_\pm(x)$ and $j_\pm(x)$ calculated for the equilibrium $p_{\rm eq}=e^{-x^2+\gamma(x)}$ are shown in Fig. 3. The peaks, corresponding to the right and left minima of the effective potential $U(x)-\gamma(x)$ in Fig. 2 are formed by the $(+)$ and $(-)$ particles (blue and red solid lines), respectively. They persist there until their flipping; the blue and red dashed lines depict the fluxes of the flipped particles to the opposite potential minimum. The net flux $j_+ + j_-$ is zero and $p_\pm$ is time independent, so the reduced dynamics records (quasi)equilibrium, but indeed, the particles circulate across the potential well flipping and moving there and back.

Similar circulating currents move the ratchet effect in the periodic but asymmetric channels, e.g., in the Feynman-Smoluchowski ratchet [30,37,38]. We also test the presence of this effect in our studied system with the trial potential

$$U(x)=2-\cos x+\eta\sin 2x; \tag{3.5}$$

the parameter $\eta$ controls its asymmetry (see Fig. 4).

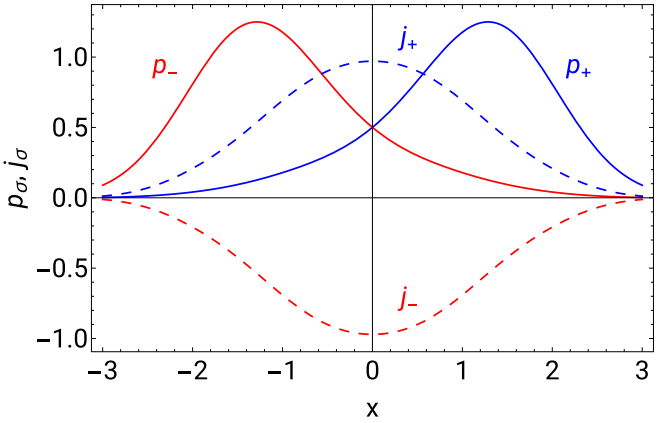


FIG. 3. Quasiequilibrium densities $p_\pm(x)$ (solid lines) and the corresponding fluxes $j_\pm(x)$ (dashed lines) of $(+)$ and $(-)$ particles, blue and red lines, respectively, for the potential $U(x)=x^2$, $\alpha=0.5$, and $f=3$.

Having the formulas for $\gamma(x)$ and $1/D(x)$, finding the rectified current in a periodic channel is straightforward. The generalized FJ equation (1.3), or its stationary version (2.15) with $\gamma(x)$ determined by our mapping, describes diffusion in a washboard (periodic) potential with a tilt given by $\Delta\gamma=\gamma(L)-\gamma(0)$. So the Stratonovich formula [39,40] is applicable:

$$J=\frac{(1-e^{-\Delta\gamma})}{\int_0^L e^{-U(x)+\gamma(x)}dx\int_x^{L+x}[e^{U(x')-\gamma(x')}/D(x')]dx'} \tag{3.6}$$

is the net flux of one particle per period $L$ in our notation. If $e^{\gamma(x)}=E(x)=1+f^2E_1(x)+\cdots$, as well as $1/D(x)=1+f^2\chi_1(x)+\cdots$ are expanded in $f^2$, Eq. (A6), we obtain the expansion of $J$ in $f^2$. Its leading term simplifies to

$$J_1=f^2[E_1(L)-E_1(0)]\left(\int_0^L e^{-U(x)}dx\int_0^L e^{U(x)}dx\right)^{-1}, \tag{3.7}$$

which is the effective force $\Delta\gamma/L=f^2[E_1(L)-E_1(0)]/L$ up to $\sim f^2$, multiplied by the linear density $1/L$ and mobility given by the Lifson-Jackson formula [41].

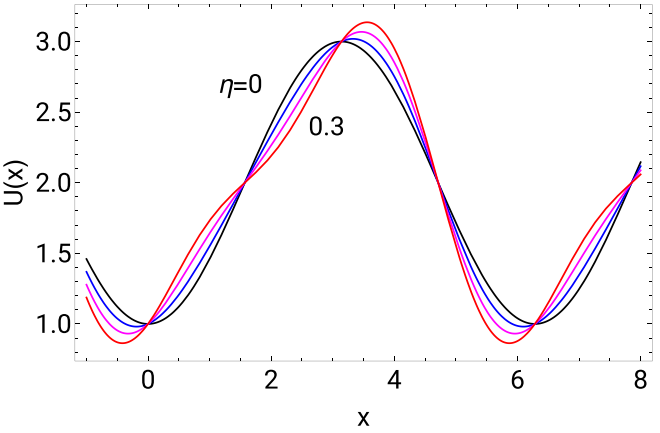


FIG. 4. Trial potential (3.5) for various parameters $\eta=0$ (black), 0.1 (blue), 0.2 (magenta), and 0.3 (red).

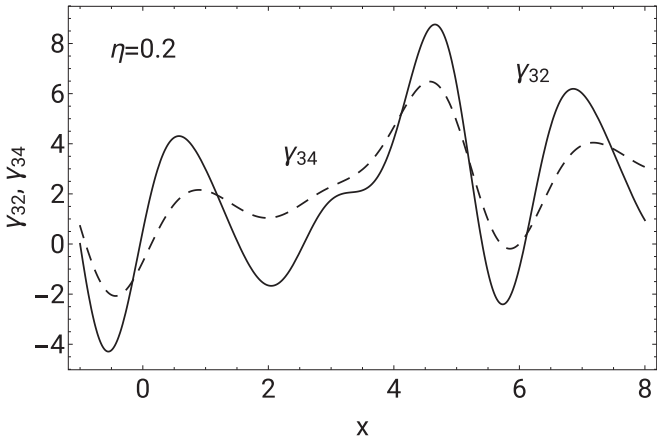


FIG. 5. Coefficients of $\gamma(x)$ at $\tau^3 f^2$ and $\tau^3 f^4$, $\gamma_{3,2}(x)$ (solid line) and $\gamma_{3,4}(x)$ (dashed line), respectively, in the potential (3.5) for $\eta = 0.2$.

Thus the key quantity determining the rectified current is increment of the gauge function $\gamma(x)$ per one period $L$. Its nonzero value can only be generated by the integral terms like those $\sim \int U'^3 dx$ and $\int U'U''^2 dx$ appearing in the third order of $\tau = 1/2\alpha$ in the expansion of $\gamma(x)$, Eq. (2.18). Let us remark that if these terms are substituted in Eq. (3.7), we recover the formula (5.18) in Ref. [28] for the ratchet driven by the fast fluctuating two-state force. For our trial potential (3.5), we get

$$-\int U'U''^2 dx = \frac{3\eta x}{2} + \frac{\cos^3 x}{3} - \frac{\eta(4\sin 2x + 5\sin 4x)}{8} + 8\eta^2\left[\cos x - \frac{\cos 5x}{5}\right] - \frac{16\eta^3}{3}\sin^3 2x,$$

$$-\int U'^3 dx = \frac{3\eta x}{2} + \text{periodic terms}.$$

Plots of the coefficients of $\gamma(x)$ standing at $\tau^3 f^2$ and $\tau^3 f^4$ depicted for $\eta = 0.2$ in Fig. 5 show the corresponding tilted contributions to the effective potential $U(x) - \gamma(x)$.

Then the increment per period $L = 2\pi$ reads

$$\Delta\gamma = \frac{3\pi\eta}{8\alpha^3}(f^2 + f^4) - \frac{9\pi\eta f^2}{8\alpha^4} + \frac{\pi\eta f^2}{32\alpha^5}(71 - 195\eta^2) + \cdots, \tag{3.8}$$

also adding the terms of $\tau^4 f^2$ and $\tau^5 f^2$ orders given by Eqs. (A9). The corresponding rectified fluxes $J$ calculated according to Eq. (3.7) (and divided by $f^2$ to emphasize the leading terms) are described in Fig. 6 as dashed lines for $f = 0.1$ (red) and $f = 1$ (blue). They are compared with numerical stationary solutions of the full problem, Eq. (1.1), green diamonds for $f = 0.1$ and blue disks for $f = 1$. Our mapping found correctly the asymptotic behavior of $J \sim 1/\alpha^3$ for large flipping rates. For small $f$ ($= 0.1$), formula (3.8) up to $\sim\tau^5$ fits well the numerical results for higher $\alpha$ ($>3$). The only included term $\sim f^4$ shifts the (blue) line for $f = 1$ in the correct direction, but taking more higher-order terms is necessary to achieve a better agreement with the numerical data (blue dots).

Nevertheless, the truncated series cannot describe $J$ correctly for smaller $\alpha$. Then instead of using Eq. (3.8), one can

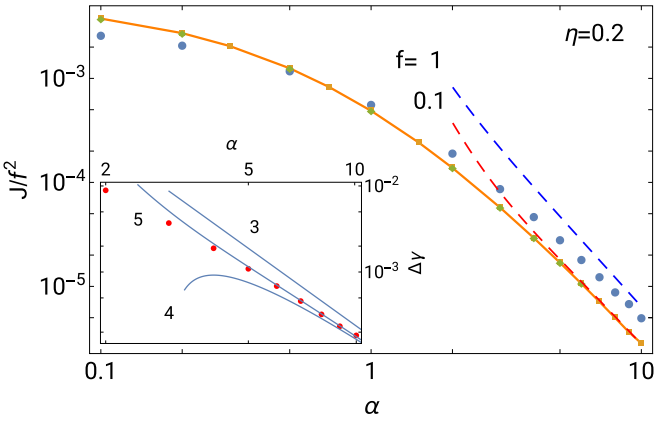


FIG. 6. Rectified current $J$ divided by $f^2$ depending on the flipping rate $\alpha$ for $\eta = 0.2$. The green diamonds and the blue dots represent the numerical stationary solution of Eq. (1.1) for $f = 0.1$ and 1, respectively. The orange line with dots depicts the flux $J_1$, Eq. (3.7) with $\Delta\gamma$ calculated from the numerical solution of Eq. (A7). In all cases, the periodicity of $p_\pm(x)$, $E_1'(x)$, and their derivatives was held. The dashed lines represent the current corresponding to Eq. (3.8) for $f = 0.1$ (red) and $f = 1$ (blue line). The inset compares $\Delta\gamma$ obtained by the numerical solution of Eq. (A7) (red dots) with the terms $\sim f^2$ in Eq. (3.8) truncated at the third, fourth, and fifth order in $1/\alpha$.

solve Eq. (3.1) for $e^{\gamma(x)}$ expanded in $f^2$, avoiding expansions in $1/\alpha$. Its leading term $E_1(x)$ [see Eq. (A7) and its solution in the Appendix] gives the current $J$ fitting correctly the solution of the full problem in the whole range of $\alpha$ for small $f$ (orange line and dots in Fig. 6). The inset of Fig. 6 documents convergence of the expansion (3.8) truncated at the third, fourth, and fifth order in $1/\alpha$ (lines, keeping only the terms $\sim f^2$); they are compared with the numerical solution of Eq. (A7) (red dots).

The effective diffusion coefficient $D(x)$ does not enter the formula for the leading term of the rectified current $J_1$, Eq. (3.7). For completeness, we also show $\chi_1(x)$ in Fig. 7, the leading correction to $1/D(x) \sim f^2$, solving numerically Eq. (A11). For larger $\alpha$, it only slightly varies around the leading value $\chi_1 \simeq -1/2\alpha$, which is the potential independent

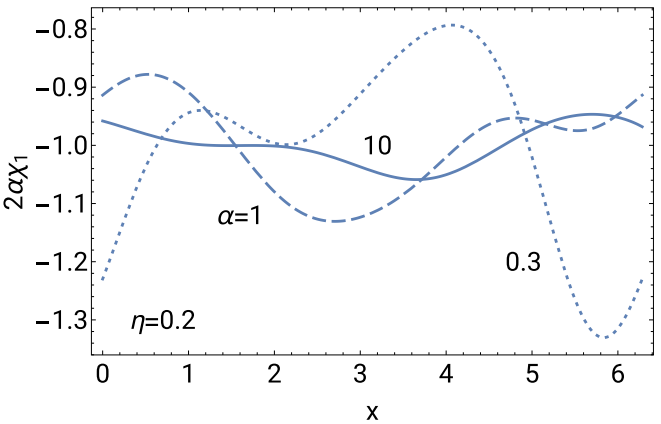


FIG. 7. The leading correction $\chi_1(x)$ in $f^2$ to the inverse effective diffusion coefficient $1/D(x)$ for the channel defined by Eq. (3.5) with $\eta = 0.2$ and various flipping rates $\alpha$.

term $\sim\tau^1$ in Eq. (2.17). This result indicates dominance of the Taylor-like dispersion [36] $D(x) \simeq 1 + f^2/2\alpha$ over the other terms depending on derivatives of the potential $U(x)$. Nevertheless, using it in calculation of the rectified current for our parameters $f$ and $\alpha$ has only a minimum impact on the results (dashed lines) depicted in Fig. 6. The rectified current $J$ for small $f$ is determined mainly by $\Delta\gamma$.

Our examples show that the reduced dynamics of 1D Janus particles offers a practical description of the phenomena expected in such systems. Piling of particles at the walls is reflected by lowering the real potential $U(x)$ by the gauge function $\gamma(x)$; the ratchet in a periodic asymmetric channel is effectively driven by the effective force $\Delta\gamma/L$ given by the increment of $\gamma(x)$ over one period $L$. Of course, the key is calculation of this function. The mapping formulated in Sec. II results in a series expanded in $1/\alpha$, which gives the correct asymptotic behavior of $\Delta\gamma$ and, thus, the rectified current $J$ for the large flipping rates. For smaller $\alpha$, one can use Eq. (3.1), which can be solved by various methods, expanding also in $f^2$, or $\alpha$, to provide validity of the results in the desired range of parameters.

## IV. CONCLUSION

Our main aim was to demonstrate the dimensional reduction of the "internal" degrees of freedom on a very simple model of 1D Janus particles driven by the self-propelling force $f$ on a line in the potential $U(x)$. Here the orientation of the particle plays the role of the transverse coordinate, which is reduced. The natural small parameter is inverse of the flipping rate $\alpha$ between two possible orientations. For infinite $\alpha$, the particles behave as passive, whose dynamics is governed by the Smoluchowski equation in the potential $U(x)$. The series of corrections in $1/\alpha$, also depending on derivatives of $U(x)$, generates finally the generalized Fick-Jacobs equation (1.3), representing the reduced dynamics.

The applied mapping technique is similar to the mapping of a 2D (passive) particle diffusing in a nonhomogeneous channel driven by the vortex force [29]. It is necessary to insert here a new gauge function $\gamma(x)$ in the operator of backward mapping $\hat{\omega}(x, \partial_x)$ and all related functions, to get the mapped equation in the form of Eq. (1.2). Finally, this function plays the role of an additional effective potential, which is subtracted from the real potential $U(x)$, and it is responsible for the peculiar effects observed in these systems.

The first one is piling of the particles at the walls, which is documented here on the example of a parabolic well. The corresponding $\gamma(x)$ decreases the real potential in a way that their (quasi)equilibrium density is increased at the soft walls. In the fine-grain picture, the new maxima of density are formed by the particles pushed against the right and left slope of the well by their self-propulsion until they randomly flip their orientation. Thus the quasiequilibrium seen by the reduced dynamics is formed by the circulating flows of the flipping particles, diffusing there or back according to their momentary orientation.

This situation resembles diffusion of particles driven by the vortex force, where similar circulating currents generate the ratchet effect in periodic asymmetric channels [30]. Indeed, our formalism approves the appearance of the ratchet current $J \sim 1/\alpha^3$ for large $\alpha$; there are integral terms in the effective potential $U(x) - \gamma(x)$, Eq. (2.18), breaking periodicity of the periodic asymmetric potential and then the increment $\Delta\gamma = \gamma(L) - \gamma(0)$ over the period $L$ represents the effective driving force of the ratchet. Our asymptotic formula (3.8) for the trial potential (3.1) works well for small $f$ and large $\alpha$ if compared with the numerical solution of the full problem, Eq. (1.1).

The general mapping method presented in Sec. II gives $\gamma(x)$ and the effective diffusion coefficient $D(x)$ expanded in $1/\alpha$, which restricts its use for only large flipping rates $\alpha$. However, the mapping algorithm can also be modified in the limit of stationary flow (see the Appendix), leading to a couple of equations for $\gamma(x)$ and $D(x)$. The solution represents summation of the series in $1/\alpha$, extending their usability in the full range of $\alpha$. For a small self-propelling force $f$, one only needs to calculate the leading term of $\gamma$ in $f^2$, as the leading term of the ratchet current is determined solely by the increment $\Delta\gamma$; $D(x)$ influences only the higher orders of $J$ in $f^2$.

Of course, the 1D model of Janus particles is too simple to describe satisfactorily the real systems of active particles; we used it rather as a toy model for demonstration of the mapping. Still, it can be understood as a simplified picture of Ozin's nanoparticles in a 2D channel of varying width $h(x)$ in the Fick-Jacobs approximation, after naive reduction of the transverse coordinate, as well as the orientation of particles onto two states: forward and backward. The width $h(x)$ is then considered as the Boltzmann weight of the entropic potential, replacing the real potential $U(x)$ in our Eq. (1.1). Another interpretation is the 1D fluctuating force ratchet [28] with passive particles driven randomly forward or backward by a force of constant amplitude $f$. The real potential $U(x)$ can also represent the electric field. However, if the Janus particle is a dipole [42], then the flipping term in Eq. (1.1) has to be modified as one of the orientations is favored in nonzero electric intensity, $-U'(x)$. We suppose that the formalism and examples introduced here will be useful for solving more complicated systems of active particles in 2D or 3D confinement in the future.

## ACKNOWLEDGMENTS

Support from VEGA Grant No. 2/0044/21 is gratefully acknowledged.

## APPENDIX: STATIONARY MAPPING

We present here an alternative mapping procedure, deriving directly the functions $D(x)$ and $\gamma(x)$. It is based on the scheme formulated in Sec. II, searching for the operator of backward mapping $\hat{\omega}(x, \partial_x)$. We found that it is composed of two parts: the first one, $\tilde{\omega}(x, \partial_x)\partial_x$, containing the derivatives $\partial_x$, and the second part, $\omega(x)$, which is just a function. They determine the operator $\hat{Z}(x, \partial_x)$ and the function $\gamma(x)$, respectively, according to Eq. (2.7). Acting on the stationary density $p_s(x)$ enables us to identify the terms composing two separate equations for $D(x)$ and $\gamma(x)$.

If $p(x, t) = p_s(x)$ is stationary, then also $p_\pm(x, t)$ calculated according to the backward mapping formula (2.4) are independent of time, so if applied in Eq. (1.1), we get zero

on the left-hand sides. Summation of the equations for both orientations gives

$$0 = \partial_x[h(x)\partial_x e^{\gamma(x)} - 2fh(x)e^{\gamma(x)}\hat{\omega}(x,\partial_x)]\frac{p_s(x)}{A(x)}; \quad \text{(A1)}$$

their subtraction results in

$$0 = (-4\alpha h e^{\gamma}\hat{\omega} + \partial_x[2h\partial_x e^{\gamma}\hat{\omega} - fhe^{\gamma}])\frac{p_s}{A}, \quad \text{(A2)}$$

omitting the obvious arguments and abbreviating $h = h(x) = e^{-U(x)}$, the Boltzmann weight of the potential $U(x)$. The first equation is the stationary mass conservation, $0 = \partial_x J$; the second one generates $1/D(x)$ and $\gamma'(x)$ after applying some tricks.

First we demonstrate the tricks on Eq. (A1), checking the identity. We use Eq. (2.7) to replace $2fhe^{\gamma}\hat{\omega}$ in Eq. (A1) by $A(\gamma' + \hat{Z}\partial_x)$, i.e.,

$$\begin{aligned} 0 &= \partial_x[he^{\gamma}(\partial_x + \gamma') - A(\gamma' + \hat{Z}\partial_x)]\frac{p_s}{A} \\ &= \partial_x[A(1-\hat{Z})]\partial_x\frac{p_s}{A} = -\partial_x J, \end{aligned}$$

which is zero for the stationary $p_s$.

In Eq. (A2), we also replace $2f\hat{\omega}$ by $\gamma' + \hat{Z}\partial_x$, and express the term $\sim\alpha$,

$$\frac{2\alpha}{f}he^{\gamma}(\gamma' + \hat{Z}\partial_x)\frac{p_s}{A} = \partial_x\left[\frac{h}{f}\partial_x e^{\gamma}(\gamma' + \hat{Z}\partial_x) - fhe^{\gamma}\right]\frac{p_s}{A}. \quad \text{(A3)}$$

The stationary $p_s$ can be formally expressed from Eq. (2.15), $p_s/A = -\int J/(AD)dx$. The net flux $J$ is irrelevant; we set $J = -1$. Then we obtain the relations

$$(1-\hat{Z})\frac{1}{AD} = \frac{1}{A}, \quad \hat{Z}\frac{1}{AD} = \hat{Z}\partial_x\frac{p_s}{A} = \frac{1}{A}\left(\frac{1}{D} - 1\right),$$

from Eq. (2.7) and use them in the next adaption of Eq. (A1),

$$\begin{aligned} &2\alpha\left[\left(\frac{1}{D} - 1\right) + A\gamma'\frac{p_s}{A}\right] \\ &= \partial_x\left[h\partial_x e^{\gamma}\left(\frac{1}{A}\left[\frac{1}{D} - 1\right] + \gamma'\frac{p_s}{A}\right) - f^2A\left(\frac{p_s}{A}\right)\right] \\ &= \partial_x h\partial_x\frac{1}{h}\left(\frac{1}{D} - 1\right) + h(e^{\gamma})''\frac{1}{AD} + [h(e^{\gamma})'']'\frac{p_s}{A} \\ &\quad + \left(\frac{\gamma'}{D}\right)' - (f^2A)'\frac{p_s}{A} - f^2A\frac{1}{AD} \end{aligned} \quad \text{(A4)}$$

after some algebra. The derivative of $p_s/A$ was everywhere expressed by $1/AD$. The terms where it remained untouched correspond to the functional part $\omega(x)$ of the operator $\hat{\omega}$, Eq. (2.7), not containing $\partial_x$. They are eliminated by setting the proper gauge $\gamma'(x)$, so these terms form the equation for $\gamma(x)$; the rest gives the equation fixing $1/D(x)$.

We begin with the equation for $\gamma$. Collecting the terms with remaining $p_s/A$, we get

$$2\alpha\gamma' = e^{U-\gamma}\partial_x e^{-U}\left(\partial_x^2 - f^2\right)e^{\gamma}. \quad \text{(A5)}$$

On one hand, we can expand now $\gamma(x)$ in the small parameter $\tau = 1/2\alpha$, Eq. (2.8). The recurrence scheme obtained by comparing the coefficients at the same powers of $\tau$ is direct and so effective. Starting with the zeroth order, $e^{\gamma} \to 1$, we recover immediately $\gamma_1' = f^2U'$, Eq. (2.11). The next orders require us to commute $e^{\gamma}$ forward to cancel $e^{-\gamma}$, retaining the lower-order coefficients of $\gamma'$ and their derivatives, recovering the results for $\gamma_n'$, Eqs. (2.13), (2.14), etc.

The second possibility of how to solve Eq. (A5) is expansion in the powers of $f^2$. Instead of $\gamma$, we rather expand

$$E(x) = e^{\gamma(x)} = 1 + \sum_{j=1}^{\infty} f^{2j}E_j(x), \quad \text{(A6)}$$

for which Eq. (A5) is homogeneous. Comparing the coefficients at the same powers of $f^2$, we obtain a simple chain generating the recursive equations for $E_j$. We focus here only at the leading term $E_1(x)$, given by the terms $\sim f^2$,

$$2\alpha e^{-U(x)}E_1'(x) = \partial_x e^{-U(x)}[\partial_x E_1'(x) - 1]. \quad \text{(A7)}$$

The solution can be expressed as

$$\begin{aligned} E_1' &= [2\alpha e^{-U} - \partial_x e^{-U}\partial_x]^{-1}(-e^{-U})' \\ &= \sum_{n=1}^{\infty}\frac{1}{(2\alpha)^n}[e^{U}\partial_x e^{-U}\partial_x]^{n-1}U'. \end{aligned} \quad \text{(A8)}$$

One can easily compare the coefficients at $1/(2\alpha)^n$ with the coefficients of $\gamma_n' \sim f^2$, Eqs. (2.11), (2.13), (2.15), etc., as $\gamma' = (\ln E)' = f^2E_1' + f^4(E_2' - E_1E_1') + \cdots$. Also it is easier to find the corresponding integral parts of $\gamma_n$ from them, Eq. (2.18), generating the effective force $\Delta\gamma/L$ in asymmetric periodic channels, driving the ratchet effect,

$$\begin{aligned} \tilde{E}_{1,3} &= -\int U'U''^2dx, \\ \tilde{E}_{1,4} &= 2\int U'(U^{(3)})^2dx, \\ \tilde{E}_{1,5} &= \int\left[U'(U'U'')'^2 - 3U'(U^{(4)})^2 - 6U''U^{(3)}U^{(4)}\right]dx, \\ &\cdots. \end{aligned} \quad \text{(A9)}$$

Collecting the terms free of $p_s/A$ in Eq. (A4), we obtain the equation for $1/D(x)$,

$$\begin{aligned} 2\alpha\left(\frac{1}{D} - 1\right) &= \partial_x e^{-U}\partial_x e^{U}\left(\frac{1}{D} - 1\right) + \frac{\gamma'' + \gamma'^2}{D} \\ &\quad + \left(\frac{\gamma'}{D}\right)' - \frac{f^2}{D}; \end{aligned} \quad \text{(A10)}$$

it requires to have $\gamma'(x)$ already calculated. If also $1/D$ is expanded in $\tau = 1/2\alpha$, comparing the terms at the same powers of $\tau$ gives a recurrence scheme, which recovers the result

(2.17). Again, one can expand $1/D(x)$ in $f^2$, too: $1/D(x) = 1 + \sum_{j=1}^{\infty} f^{2j}\chi_j(x)$. Expressing $\gamma = \ln E$ in Eq. (A10) and expanding it in $f^2$ [with use of Eq. (A6)], we find recurrence relations for the coefficients $\chi_j$. The leading correction is given by

$$2\alpha\chi_1 = \partial_x e^{-U}\partial_x e^{U}\chi_1 - 1 + 2E_1''. \tag{A11}$$

If expanded also in $\tau$, it reproduces the coefficients $\sim f^2$ of $1/D(x)$ in Eq. (2.17).


[1] H. C. Berg and L. Turner, Biophys. J. **58**, 919 (1990).
[2] W. R. DiLuzio, L. Turner, M. Mayer, P. Garstecki, D. B. Weibel, H. C. Berg, and G. M. Whitesides, Nature (London) **198**, 1271 (2005).
[3] P. Galajda, J. Keymer, P. Chaikin, and R. Austin, J. Bacteriol. **189**, 8704 (2007).
[4] B. M. Friedrich, I. H. Riedel-Kruse, J. Howard, and F. Jülicher, J. Exp. Biol. **213**, 1226 (2010).
[5] J. R. Howse, R. A. L. Jones, A. J. Ryan, T. Gough, R. Vafabakhsh, and R. Golestanian, Phys. Rev. Lett. **99**, 048102 (2007).
[6] U. M. Cordova-Figueroa and J. F. Brady, Phys. Rev. Lett. **100**, 158303 (2008).
[7] M. N. Popescu, S. Dietrich, and G. Oshanin, J. Chem. Phys. **130**, 194702 (2009).
[8] L. F. Valadares, Yu-Guo Tao, N. S. Zacharia, V. Kitaev, F. Galembeck, R. Kapral, and G. A. Ozin, Small **6**, 565 (2010).
[9] M. Schmitt and H. Stark, Europhys. Lett. **101**, 44008 (2013).
[10] J. P. Hernandez-Ortiz, C. G. Stoltz, and M. D. Graham, Phys. Rev. Lett. **95**, 204501 (2005).
[11] M. Paoluzzi, R. Di Leonardo and L. Angelani, Phys. Rev. Lett. **115**, 188303 (2015).
[12] P. Hänggi and F. Marchesoni, Rev. Mod. Phys. **81**, 387 (2009).
[13] L. Angelani, A. Costanzo and R. Di Leonardo, Europhys. Lett. **96**, 68002 (2011).
[14] P. Malgaretti, I. Pagonabarraga, and J. M. Rubí, Front. Phys. **1**, 21 (2013).
[15] P. Malgaretti, I. Pagonabarraga, and J. M. Rubí, J. Chem. Phys. **138**, 194906 (2013); Eur. Phys. J.: Spec. Top. **223**, 3295 (2014).
[16] P. K. Ghosh, V. R. Misko, F. Marchesoni, and F. Nori, Phys. Rev. Lett. **110**, 268301 (2013).
[17] B.-q. Ai, Q.-y. Chen, Y.-f. He, F.-g. Li, and W.-r. Zhong, Phys. Rev. E **88**, 062129 (2013).
[18] M. H. Jacobs, *Diffusion Processes* (Springer, New York, 1967).
[19] R. Zwanzig, J. Phys. Chem. **96**, 3926 (1992).
[20] D. Reguera and J. M. Rubí, Phys. Rev. E **64**, 061106 (2001).
[21] P. Kalinay and J. K. Percus, J. Chem. Phys. **122**, 204701 (2005).
[22] P. Kalinay and J. K. Percus, J. Stat. Phys. **123**, 1059 (2006).
[23] P. Kalinay and J. K. Percus, Phys. Rev. E **74**, 041203 (2006).
[24] S. Martens, G. Schmid, L. Schimansky-Geier, and P. Hänggi, Phys. Rev. E **83**, 051135 (2011); Chaos **21**, 047518 (2011).
[25] P. Kalinay, Phys. Rev. E **80**, 031106 (2009).
[26] P. Kalinay and J. K. Percus, Phys. Rev. E **83**, 031109 (2011).
[27] P. Kalinay, Phys. Rev. E **84**, 011118 (2011).
[28] P. Reimann, Phys. Rep. **361**, 57 (2002).
[29] P. Kalinay and F. Slanina, J. Phys.: Condens. Matter **30**, 244002 (2018).
[30] P. Kalinay and F. Slanina, Phys. Rev. E **98**, 042141 (2018).
[31] J. Elgeti and G. Gompper, Europhys. Lett. **101**, 48003 (2013).
[32] M. Sandoval and L. Dagdug, Phys. Rev. E **90**, 062711 (2014).
[33] E. Yariv and O. Schnitzer, Phys. Rev. E **90**, 032115 (2014).
[34] P. Malgaretti and H. Stark, J. Chem. Phys. **146**, 174901 (2017).
[35] M. Kahlen, A. Engel, and Ch. Van den Broeck, Phys. Rev. E **95**, 012144 (2017).
[36] E. Aurell and S. Bo, Phys. Rev. E **96**, 032140 (2017).
[37] A. Ryabov, V. Holubec, M. H. Yaghoubi, M. Varga, M. E. Foulaadvand, and P. Chvosta, J. Stat. Mech.: Theory Exp. (2016) 093202.
[38] V. Holubec, A. Ryabov, M. H. Yaghoubi, M. Varga, A. Khodaee, M. E. Foulaadvand, and P. Chvosta, Entropy **19**, 119 (2017).
[39] R. L. Stratonovich, Radiotekh. Elektron. **3**, 497 (1958).
[40] P. Reimann, C. Van den Broeck, H. Linke, P. Hänggi, J. M. Rubi, and A. Pérez-Madrid, Phys. Rev. E **65**, 031104 (2002).
[41] S. Lifson and J. L. Jackson, J. Chem. Phys. **36**, 2410 (1962).
[42] S. J. de Carvalho, R. Metzler, and A. G. Cherstvy, Phys. Chem. Chem. Phys. **16**, 15539 (2014).